Electron-impact excitation of neon at intermediate energies

Oleg Zatsarinny and Klaus Bartschat
Department of Physics and Astronomy, Drake University, Des Moines, Iowa 50311, USA
(Received 18 July 2012; published 30 August 2012)

Large-scale R matrix with pseudostates calculations for electron collisions with neon atoms, using a recently developed parallel version of our B-spline R-matrix code, are reported. The calculations were carried out in the jK-coupling scheme. They are intended to provide converged (with respect to the number of coupled states) results for electron impact excitation of individual target states with dominant configurations $2p^5 3s$, $2p^5 3p$, and $2p^5 3d$ for incident electron energies from threshold to 300 eV. The close-coupling expansion includes 457 target states, with the lowest 87 states representing the bound spectrum and the remaining 370 the ionization continuum. The results reveal dramatic reductions of the predicted excitation cross sections at intermediate energies due to a strong influence of coupling to the target continuum and the higher-lying Rydberg states. Comparison with available experimental data for the excitation of the $2p^5 3s$ and $2p^5 3p$ states raises questions about the absolute normalization in the measurements. Considerable improvement over previous work is obtained in the agreement between experiment and theory for the angle-differential cross sections. In particular, a long-standing discrepancy regarding the angular dependence for excitation of the metastable $2p^5 3s$ levels is resolved.

DOI: 10.1103/PhysRevA.86.022717 PACS number(s): 34.80.Dp

I. INTRODUCTION

Electron-impact excitation of neon has many applications in different areas such as gaseous electronics, astrophysics, and controlled nuclear fusion. On the fundamental side, many measurements and calculations for angle-integrated and angle-differential electron-impact excitation cross sections of neon have been carried out. To name just a few, a 31-state semirelativistic R-matrix (close-coupling) calculation was performed by Zeman and Bartschat [1] with the principal goal of describing excitation from the $(2p^6)^1S$ ground state to the levels of the $2p^5 3s$ and $2p^5 3p$ configurations, measurements of the angle-integrated cross sections from the ground state to the levels of the $2p^5 3p$ configuration were carried out by Chilton *et al*. [2], measurements for excitation out of the two metastable states with configuration $2p^5 3s$ to selected levels of the $2p^5 3p$ configuration were reported by Boffard *et al*. [3], and a joint experimental and theoretical study of integrated (ICS) and differential (DCS) cross sections from the ground state to the levels of the $2p^5 3s$ was performed by Khakoo *et al*. [4].

Despite the importance of the e-Ne collision system and the significant efforts devoted to it, the overall agreement between experiment and theory at low and intermediate energies (up to a few times the ionization threshold) is far from satisfactory. As shown, for example, by Khakoo *et al*. [4], none of the many theoretical methods was able to consistently reproduce the experimental data for the angle-differential cross sections for excitation of the $2p^5 3s$ states, or their ratios, which represent a very sensitive test to the quality of the theoretical model.

For incident energies in the vicinity of the lowest few excitation thresholds, significant progress was finally achieved by means of the B-spline R-matrix method [5]. The key feature of this method is the possibility to employ *nonorthogonal* sets of term-dependent one-electron orbitals. This allows for more accurate target descriptions than those used in previous collision calculations. Excellent agreement with experiment was observed, for instance, in the energy dependence of the cross sections for the production of metastable Ne atoms in a 31-state B-spline R-matrix model [6], to be referred to as BSR-31 below. The predicted resonance structure was subsequently confirmed experimentally [7]. Very good agreement at low energies was also achieved between experiment and theory in the energy dependence of the DCS for excitation of the $2p^5 3s$ and $2p^5 3p$ states [8,9].

Even though the BSR-31 calculations described the low-energy resonance structure and the energy dependence of various scattering parameters very accurately, these calculations did not include coupling to the target continuum. (Below we will generally refer to "continuum coupling" for brevity of notation, although strictly speaking this coupling also includes the high-lying Rydberg states.) Consequently, they cannot be considered fully converged regarding, in particular, the absolute values of the excitation cross sections. Furthermore, it is likely that the problem is exacerbated at "intermediate" energies up to a few times the ionization threshold. In fact, the importance of coupling to the target continuum in calculating electron impact excitation of neon was demonstrated by Ballance and Griffin [10], who predicted that this coupling can reduce the theoretical cross section by factors of up to 5, especially for nondipole, optically forbidden transitions. Due to the available computational resources at the time, however, Ballance and Griffin could only obtain reasonably converged results in a nonrelativistic LS-coupling scheme. Such a scheme, on the other hand, is known to be inappropriate for most excited states in neon, which should be described at least in a semirelativistic intermediate coupling framework.

Another indication, albeit indirect, was obtained in a joint experimental and theoretical study of a neon plasma dc discharge [11,12], where the electron energy distribution function in the positive column was reconstructed from optical emission spectroscopic data. The plasma and the spectroscopic measurement were modeled by employing a complete and consistent set of atomic structure and electron collision data generated in the early BSR-31 calculations [6].

The probabilistic nature of the approach made it possible to account for estimated uncertainties in the atomic data set and to check the consistency of the model with these errors given. When the uncertainties of the BSR-31 excitation cross sections were estimated as 10–20% for the $2p^5 3s$ states, 40% for the $2p^5 3p$ states, and 60% for the $2p^5 3d$ states, inconsistencies appeared that suggested too small error estimates particularly for the $2p^5 3d$ case. The problems included the optically allowed $2p \rightarrow 3d$ one-electron excitations to states with total electronic angular momentum $J = 1$ and hence came as a major surprise. Unfortunately, no direct test of the theoretical predictions has yet been carried out with the crossed-beam technique, due to the difficulties associated with such measurements.

The purpose of the present work is to extend our recent nonrelativistic calculations [13] to include relativistic effects at the level of the semirelativistic Breit-Pauli approximation. Given today's state-of-the-art supercomputer facilities, we expect to obtain converged (with the number of states in the close-coupling expansion) results for state-to-state excitation cross sections in the appropriate intermediate coupling scheme for the target states of neon. Such converged results could not yet be obtained by Ballance and Griffin [10], due to the lack of computational power at the time. In Sec. II, we briefly summarize our computational model. This is followed in Sec. III by a comparison with a variety of experimental data for angle-integrated (Sec. III A) and angle-differential (Sec. III B) cross sections. We finish with a short summary and conclusions in Sec. IV.

II. COMPUTATIONAL DETAILS

The target-structure calculations and the scattering calculations in the present work are very similar to our recent nonrelativistic R-matrix with pseudostates (RMPS) calculations [13]. Hence we only highlight the most important aspects of, as well as the few differences between, these two computational models. In the present work, we employ the Breit-Pauli Hamiltonian to account for relativistic effects, which manifest themselves predominantly in a large spin-orbit mixing of different LS terms. Except for very few states, e.g., the metastable $(2p^5 3s)^3P_{2,0}$ states, $(2p^5 3p)^3 D_3$, or $(2p^5 3d)^3 F_4$, LS coupling does not provide a good representation for neon. The excited levels therefore are usually designated in the jK-coupling scheme [14].

The neon target states were generated by combining the multiconfiguration Hartree-Fock and the B-spline box-based multichannel methods [15]. The structure of the multichannel target expansion was chosen the same as in the LS calculations [13]. It includes the $2s^2 2p^5 nl$ and $2s2p^6 nl$ Rydberg series of bound states in Ne, as well as continuum pseudostates lying above the ionization limit. Inner-core (short-range) correlations are included through the configuration interaction (CI) expansion of the corresponding ionic states.

In our atomic-structure calculations for noble gases [16], we found that core-valence correlation corrections are very important for an accurate representation of the excited $2p^5 nl$ states, and this correlation can be taken into account by including core-excited configurations. That was, indeed, done in our BSR-31 calculations [6] for e-Ne collisions and resulted in very accurate excitation energies of the target states included in the close-coupling expansion. In the present calculations with many more states, we decided to omit the core-valence correlation, since it would have doubled the size of the target expansions and made the subsequent scattering calculations too extensive. The present expansions in jK coupling contained between 80 and 140 configurations for each state. Although still a challenge, such expansions can be handled with our available computational resources in the subsequent large-scale collision calculations. As seen from Table I, the excitation energies for all physical bound states differed by no more than 0.2 eV from experiment. This is considered sufficiently accurate for the intermediate-energy scattering calculations, i.e., when the projectile energy is relatively far away from the near-threshold resonance regime.

Another assessment of the quality of our target description can be obtained by comparing the results for the oscillator strengths. For the principal resonance transitions from the ground state to the $2p^5 3s'[1/2]_1$ and $2p^5 3s[3/2]_1$ states, for example, our oscillator strengths are 0.151 and 0.0148, respectively, while the experimental values are 0.156 and 0.0128 [18]. We see good agreement for the strong dipole transition to the $3s'[1/2]_1$ state with its predominant $^1P_1$ character, but about a 20% difference for the weaker intercombination transition to the $2p^5 3s[3/2]_1$ ($^3P_1$) state. This will affect the angle-integrated excitation cross section for this transition at high energies, as well as the differential cross sections at small scattering angles (see below).

The scattering calculations were carried out in the framework of the R-matrix method. We employed a newly developed, fully parallelized version of the BSR complex [5]. The R-matrix radius was set to $30\,a_0$, where $a_0 = 0.529 \times 10^{-10}$ m is the Bohr radius. We employed 70 B-splines to span this radial range using a semiexponential grid of knots. The maximum interval in this grid is $0.5\,a_0$, which is sufficient for electron scattering energies up to 300 eV. We calculated partial waves for total electronic (spin plus orbital) angular momenta $J \leqslant 50.5$ numerically and then used a top-up procedure to estimate the contribution to the transition matrix elements from even higher J values. The calculation for the external region was performed with the STGF program [19].

Our close-coupling expansion includes 457 states of neon, with the lowest 87 states representing the bound spectrum and the remaining 370 the target continuum. We included all $2s^2 2p^5 nl$ and $2s2p^6 nl$ states with $l = 0$–4. This model will be referred to as BSR-457 below. The continuum pseudostates in the present Breit-Pauli model cover the energy region up to 50 eV. This is less than in our corresponding LS calculations [13], due to the much increased complexity associated with the intermediate-coupling scheme. The present scattering model contained up to 2260 scattering channels, which is similar to the maximum number of channels in the LS calculations (2280). For a given B-spline basis, this number defines the size of the matrices involved. In the present work it leads to generalized eigenvalue problems (for each partial-wave symmetry) with matrix dimensions up to 150 000. Matrices of such dimensions can be handled with our current computational resources. Without describing the model in detail, it was already used very successfully for the calculations presented in a recent joint experimental and

TABLE I. Energy levels of the most relevant discrete Ne levels for the present work, their respective thresholds for excitation from the ground state, and the difference between experiment [17] and the present theoretical description.

State	Theory absolute (a.u.)	Theory excitation (eV)	Experiment excitation (eV)	Difference (eV)
$(2p6)^1S_0$	−128.9064982	0	0	0
$3s[3/2]_2$	−128.2888001	16.807	16.619	0.188
$3s[3/2]_1$	−128.2868780	16.860	16.671	0.189
$3s'[1/2]_0$	−128.2850872	16.908	16.715	0.193
$3s'[1/2]_1$	−128.2807954	17.025	16.848	0.177
$3p[1/2]_1$	−128.2280214	18.461	18.382	0.079
$3p[5/2]_3$	−128.2219448	18.627	18.555	0.072
$3p[5/2]_2$	−128.2211681	18.648	18.576	0.072
$3p[3/2]_1$	−128.2198310	18.684	18.613	0.071
$3p[3/2]_2$	−128.2190237	18.706	18.637	0.069
$3p'[3/2]_1$	−128.2168761	18.765	18.693	0.054
$3p'[3/2]_2$	−128.2164179	18.777	18.704	0.084
$3p[3/2]_0$	−128.2162728	18.781	18.711	0.077
$3p'[1/2]_1$	−128.2156808	18.797	18.726	0.071
$3p'[1/2]_0$	−128.2075561	19.018	18.966	0.052
$4s[3/2]_2$	−128.1822914	19.706	19.664	0.042
$4s[3/2]_1$	−128.1814190	19.729	19.688	0.041
$4s'[1/2]_0$	−128.1785799	19.807	19.761	0.046
$4s'[1/2]_1$	−128.1779087	19.825	19.780	0.045
$3d[1/2]_0$	−128.1701388	20.036	20.025	0.011
$3d[1/2]_1$	−128.1700778	20.038	20.026	0.012
$3d[7/2]_4$	−128.1697778	20.046	20.035	0.011
$3d[7/2]_3$	−128.1697632	20.047	20.035	0.012
$3d[3/2]_2$	−128.1696994	20.048	20.037	0.011
$3d[3/2]_1$	−128.1695844	20.051	20.040	0.011
$3d[5/2]_2$	−128.1692919	20.059	20.048	0.011
$3d[5/2]_3$	−128.1692794	20.060	20.048	0.012
$3d'[5/2]_1$	−128.1658949	20.152	20.136	0.016
$3d'[5/2]_3$	−128.1658814	20.152	20.136	0.016
$3d'[3/2]_2$	−128.1658461	20.153	20.138	0.015
$3d'[3/2]_1$	−128.1657821	20.155	20.139	0.016

theoretical study on the coherence parameters measured in electron-photon coincidence setups [20].

III. RESULTS

A. Angle-integrated cross sections

The angle-integrated cross sections (ICSs) for excitation of the four $2p^5 3s$ states are presented in Fig. 1 over an extended energy range up to 300 eV. We compare our new results with those from the 31-state B-spline R-matrix calculation (BSR-31) [6] and with available experimental data. In order to demonstrate the convergence of the cross sections, we also show five-state results (BSR-5), which are expected to be close to what one might obtain in a distorted-wave approximation with the same target description. The differences between the BSR-5 and BSR-31 results illustrate the effects of coupling to the higher-lying bound states of Ne. This coupling considerably reduces the theoretical cross sections near the maximum and is responsible for the resonance structure at low energies. The effects of coupling to the continuum, represented by the differences between the BSR-31 and BSR-457 results, are even more significant. The pseudostates in the expansion not only

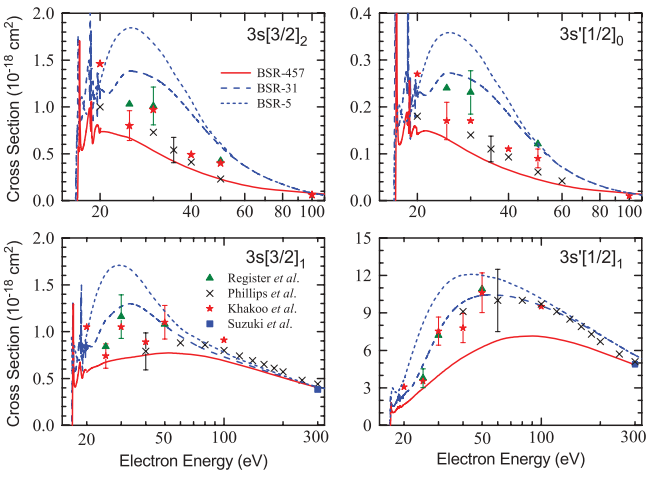

FIG. 1. (Color online) Angle-integrated cross sections for electron-impact excitation of the $2p^5 3s$ states in neon from the ground state $(2p^6)^1S_0$. The current BSR-457 results are compared with those from the BSR-5 and BSR-31 models, as well as the experimental data from Khakoo *et al.* [4], Register *et al.* [21], Phillips *et al.* [22], and Suzuki *et al.* [23].

further reduce the predicted cross sections but also change their energy dependence. The discrete-state-only R-matrix cross sections rise rapidly just above the ionization limit, while the results obtained with the pseudostates included do not. Although the most significant effects of continuum coupling occur above the ionization limit, they persist down into the bound-state energy region.

The agreement between the present results and various experimental data is rather scattered. Although we designate the $2p^5 3s$ levels in the jK-coupling scheme, they are still reasonably well described in the LS-coupling representation. This is particularly true for the metastable $3s[3/2]_2$ and $3s'[3/2]_0$ levels with dominant (nearly 100%) $^3P_2$ and $^3P_0$ character, respectively. Consequently, the excitation cross sections for these two states clearly exhibit the typical "exchange" character, dropping quickly as $1/E^3$ at high energies. In contrast to the previous calculations, our new BSR-457 results lie below the experimental values. The closest agreement is with the early measurements of Phillips *et al.* [22], which were based on the optical method employing the laser-induced fluorescence technique. The principal uncertainty in such measurements originates from extracting the cascade contributions from the measured apparent excitation cross sections. Register *et al.* [21] and Khakoo *et al.* [4], on the other hand, measured differential cross sections (DCSs) at fixed energies in crossed-beam setups. These DCSs were extrapolated to 0° and 180° and then integrated to yield absolute excitation cross sections as a function of incident electron energy. Uncertainties in this method necessarily arise from the unknown behavior of the DCS at small and large scattering angles, especially if somewhat questionable theoretical predictions are used as a guide. These uncertainties are almost certainly responsible for the scatter in the energy dependence of the experimental ICSs. We will further comment on the Khakoo *et al.* [4] data below.

As seen from Fig. 1, coupling to the continuum is even important for the strong dipole-allowed transition to the $3s'[1/2]_1(^1P_1)$ level, and its influence persists over a large range of electron energies. Here the experimental cross sections appear to be in good agreement with the BSR-31 predictions and hence exceed the new BSR-457 results by 20–40% at intermediate energies from 30 to 150 eV. New measurements, however, are currently in progress at Sophia University [24], and preliminary results suggest smaller cross sections at 100 and 200 eV than the data shown in Fig. 1. All scattering models agree with the experimental data of Suzuki *et al.* [23] at 300 eV, where the coupling effects are expected to be small.

The best agreement with the experimental data is found for excitation of the $3s[3/2]_1(^3P_1)$ level. The cross section for this level is affected by a small mixing with the $3s'[1/2]_1(^1P_1)$ level. At low energies, therefore, its variation with energy resembles that of a spin-forbidden transition, but then it transforms to the characteristics of a dipole-allowed transition at higher energies. For energies $E \geqslant 100$ eV, all scattering models provide very similar results and agree well with the available experimental data. At lower energies, we see good agreement between the BSR-457 results and experiment at 25 and 40 eV, while the experimental data of [4] and [21] at 30 and 50 eV are significantly larger than our predictions. On the other hand,

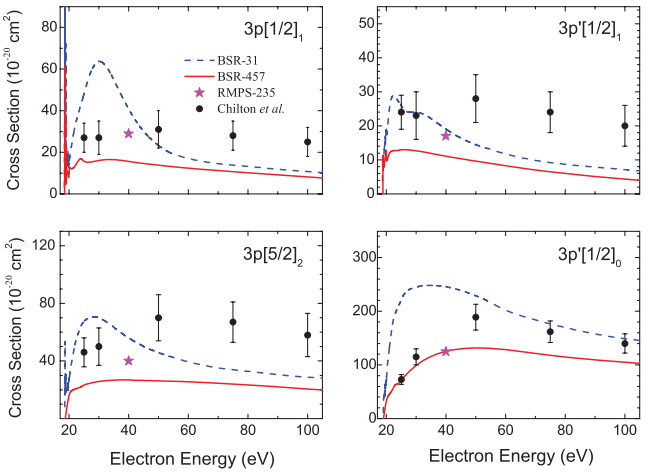

FIG. 2. (Color online) Angle-integrated cross sections for electron-impact excitation of selected states from the $2p^5 3p$ manifold in neon from the ground state $(2p^6)^1S_0$. The current BSR-457 results are compared with results from the BSR-31 [6] and RMPS-235 [10] models, and the experimental data of Chilton *et al.* [2].

there is no obvious physical reason for the scatter in these measured excitation cross sections at such high energies, and hence some of the experimental data are much further off from theory than others.

Figure 2 shows angle-integrated cross sections for electron-impact excitation of four selected $2p^5 3p$ states in neon from the $(2p^6)^1S_0$ ground state. The current BSR-457 results are compared with the BSR-31 predictions [6] and with the experimental data of Chilton *et al.* [2]. Also shown is one representative point from the RMPS-235 calculation by Ballance and Griffin [10]. We chose only one point from this work, since the results contained unphysical oscillations due to the insufficient number of states that could be handled at the time. The point depicted is a reasonable estimate of those results after smoothing out the oscillations.

In the experiment, Chilton *et al.* [2] measured the optical excitation function and then obtained the direct excitation cross section by subtracting the estimated cascade contribution. The BSR-457 cross sections lie well below the experimental values. This may, at least in part, be attributed to experimental uncertainties in defining the cascade contributions. Note, however, that the energy dependence of the BSR-457 cross sections differs drastically from that of the previous BSR-31 results and agrees much better with experiment. Including the pseudostates smoothens out the near-threshold maxima and the cross sections show a flat energy dependence over a wide range of incident energies. The continuum coupling effects are large, especially for energies right above the ionization threshold. The differences between the BSR-31 and BSR-457 results at high energies can be attributed to the different target wave functions used in these calculations.

Figure 3 depicts examples for excitation of selected states of the $2p^5 3d$ manifold in neon from the ground state. In our previous LS-coupling calculations, a large reduction in the theoretical cross sections due to continuum-coupling effects was found for these states. Since there are no experimental data available for comparison, we present a more detailed

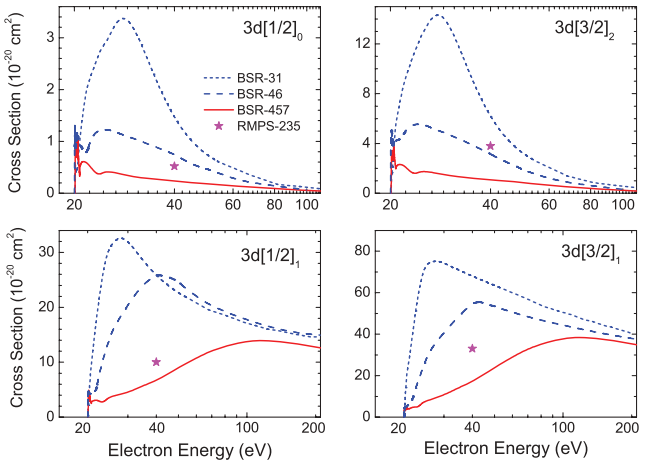

FIG. 3. (Color online) Angle-integrated cross sections for electron-impact excitation of selected states from the $2p^5 3d$ manifold in neon from the ground state $(2p^6)^1S_0$. The current BSR-457 results are compared with results from the BSR-31 and BSR-46 models. Also shown is one representative point from the RMPS-235 model [10].

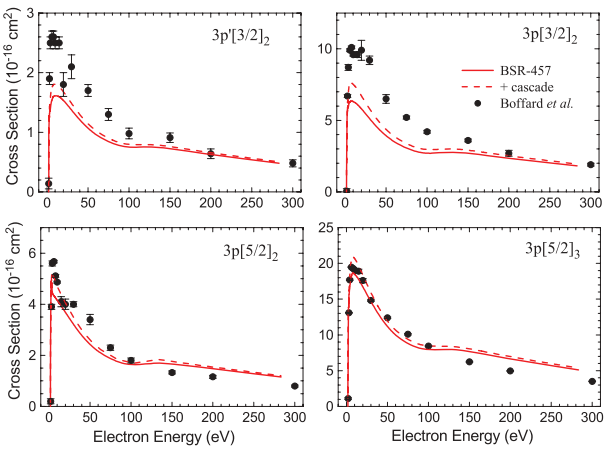

FIG. 4. (Color online) Angle-integrated cross sections for electron-impact excitation of selected states from the $2p^5 3p$ manifold in neon from the metastable $3s[3/2]_2$ level. The current BSR-457 results with and without cascade contribution are compared with the experimental data of Boffard *et al.* [3]. The experimental error bars are only statistical and do not include an overall 30% uncertainty in the absolute calibration.

discussion regarding the convergence of the close-coupling expansion in these cases. Besides the BSR-31 cross sections, we also show the results from a BSR-46 scattering model, which contains the $2p^5 4p$ and $2p^5 5s$ target states that lie just above the $2p^5 3d$ states. As seen from the figure, the $2p^5 3d$ cross sections exhibit a tremendous reduction in the intermediate energy regime with increasing size of the close-coupling expansion. A large part of this reduction, especially for the dipole-forbidden transitions, is due to the inclusion of the $2p^5 4p$ and $2p^5 5s$ bound states. For dipole-allowed transitions, on the other hand, coupling to the continuum has a more pronounced effect that persists over a wide range of incident energies. Recall that our present continuum pseudostates only cover the region up to 50 eV. We thus expect a further reduction in the theoretical cross section at higher energies if even more pseudostates were included in the close-coupling expansion. Once again we show a representative point from the early RMPS-235 work [10], which supports our predicted reduction. We also recall that there is strong, albeit indirect, evidence from the modeling of a neon plasma discharge [11,12], which suggested that our BSR-31 results for these transitions are significantly too large.

As our final example for angle-integrated cross sections, Fig. 4 exhibits a comparison of our results for electron-impact excitation of selected $2p^5 3p$ levels from the metastable state $3s[3/2]_2$ with the experimental data of Boffard *et al.* [3]. These measurements are also based on the optical method and hence determine apparent cross sections that contain cascade contributions. As seen from the figure, we predict the cascade contribution to be relatively small for excitation out of the metastable levels. This is very different from the case of excitation from the ground state to levels of the $2p^5 3p$ configuration, where the cascade contribution at some energies may even exceed the direct excitation cross section [2]. The reason for the difference is the fact that all excitations of the $2p^5 3p$ levels shown in Fig. 4 correspond to dipole-allowed transitions with small energy transfer from the metastable initial state, and such transitions should have large cross sections. Cascades into these levels mainly arise from the $2p^5 4s$ and $2p^5 3d$ configurations, but excitation of these levels from the metastable $3s[3/2]_2$ state should be small because of their dipole-forbidden nature. The overall agreement between experiment and our BSR-457 results is certainly satisfactory, especially in light of the experimental uncertainty ($\pm 30\%$) in the absolute normalization. We do not show our previous BSR-31 results here, since they are only available for small energies $E \leqslant 30$ eV and differ from the current BSR-457 results by no more than 15%. This supports the expectation of a small effect of continuum coupling for the excitation of such strong transitions.

B. Angle-differential cross sections

Figures 5–8 present results for the angle-differential cross sections for electron-impact excitation of the $2p^5 3s$ states in neon for incident projectile energies of 30, 40, 50, and 100 eV. The current BSR-457 results are compared with the experimental data of Khakoo *et al.* [4]. At 30 and 40 eV we also compare with our previous BSR-31 results [6]. Note that the experimental data were renormalized to yield good visual agreement with the BSR-457 results. The corresponding normalization coefficients indicated in the figures are the same for all $2p^5 3s$ states at a given scattering energy. In contrast to the BSR-31 predictions, we now see excellent agreement between the BSR-457 results and the experimental DCSs as a function of the scattering angle. The current calculations correctly reproduce all the minima and maxima for both the spin-forbidden and the dipole-allowed transitions. There is a striking improvement over the BSR-31 results, once again stressing the importance of coupling to the continuum. As expected, the latter is particularly important for excitation of the metastable $3s[3/2]_2$ and $3s'[1/2]_0$ states. As discussed in detail by Khakoo *et al.* [4], no previous calculation could

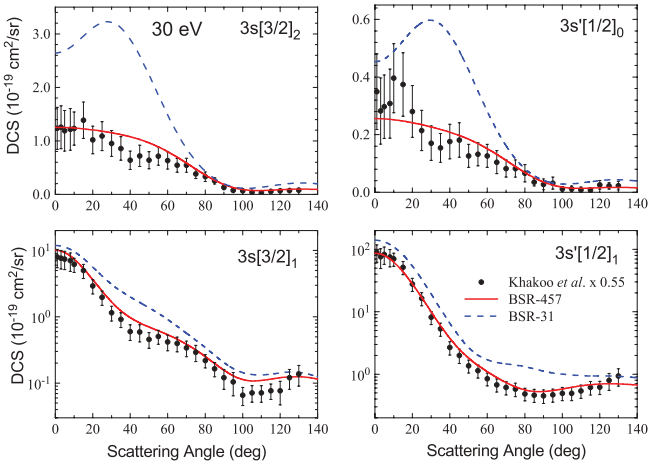

FIG. 5. (Color online) Angle-differential cross sections for electron-impact excitation of the $2p^5 3s$ states in neon from the ground state $(2p^6)^1S_0$ at an incident projectile energy of 30 eV. The present BSR-457 results are compared with the BSR-31 predictions [6] and the experimental data of Khakoo *et al.* [4]. The experimental data were renormalized by a factor of 0.55.

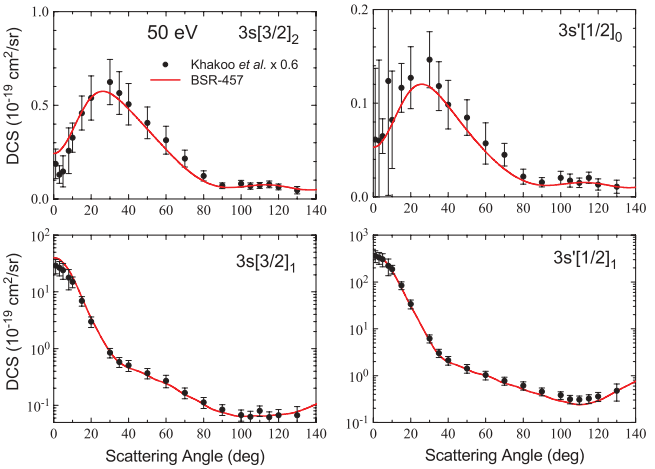

FIG. 7. (Color online) Angle-differential cross sections for electron-impact excitation of the $2p^5 3s$ states in neon from the ground state $(2p^6)^1S_0$ at an incident projectile energy of 50 eV. The present BSR-457 results are compared with the experimental data of Khakoo *et al.* [4]. The experimental data were renormalized by a factor of 0.6.

reproduce the measured angular dependence of the DCSs for the metastable states. The present results clearly confirm our earlier suggestion [6] that the results for these optically forbidden transitions are very sensitive to the inclusion of pseudostates.

Looking back at Fig. 1, it is not surprising that we suggest renormalization factors of less than unity for the experimental DCSs, except for the projectile energy of 100 eV. Here the agreement with experiment as published is good for all angles. Nevertheless, the experimental angle-integrated cross sections for the dipole-allowed transitions exceed the BSR-457 results by approximately 30% at this energy. This rather large discrepancy originates from the small-angle region $\theta \leqslant 10\%$, where extrapolated rather than actually measured values were used. The steep increase of the DCS towards forward scattering angles for these cases may be an additional source of uncertainty for the absolute normalization of the experimental data.

Figures 9 and 10 present results for the DCS ratios,

$$r \equiv \mathrm{DCS}(3s[3/2]_2)/\mathrm{DCS}(3s[1/2]_0), \quad (1)$$

$$r' \equiv \mathrm{DCS}(3s[3/2]_1)/\mathrm{DCS}(3s'[1/2]_1), \quad (2)$$

$$r'' \equiv \mathrm{DCS}(3s[3/2]_2)/\mathrm{DCS}(3s'[1/2]_1), \quad (3)$$

measured by Khakoo *et al.* [4]. As expected, the ratio r remains close to the statistical value of 5, although both experiment and theory show small deviations from it at some angles. Given the scatter in the experimental data, it is difficult to draw definite conclusions about possible trends. The experiment

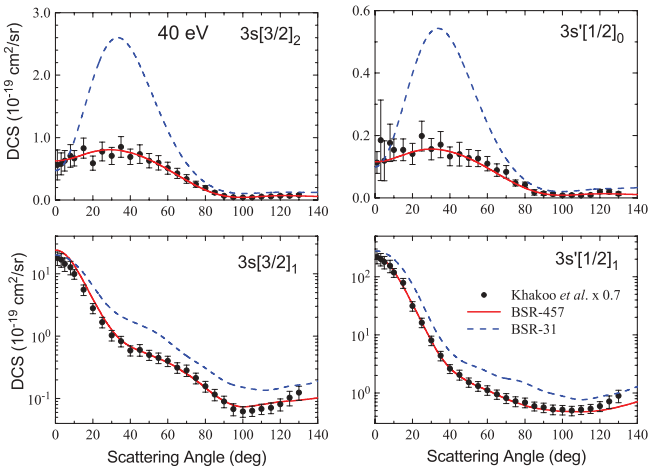

FIG. 6. (Color online) Same as Fig. 5 for an incident projectile energy of 40 eV. The experimental data were renormalized by a factor of 0.7.

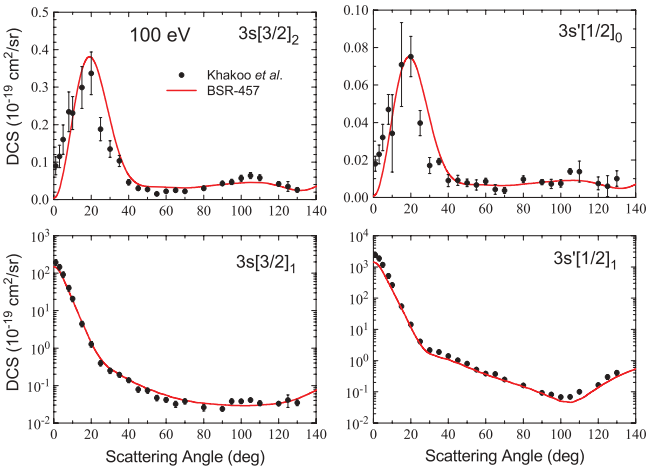

FIG. 8. (Color online) Same as Fig. 7 for an incident projectile energy of 100 eV. No renormalization factor for the experimental data was applied in this case.

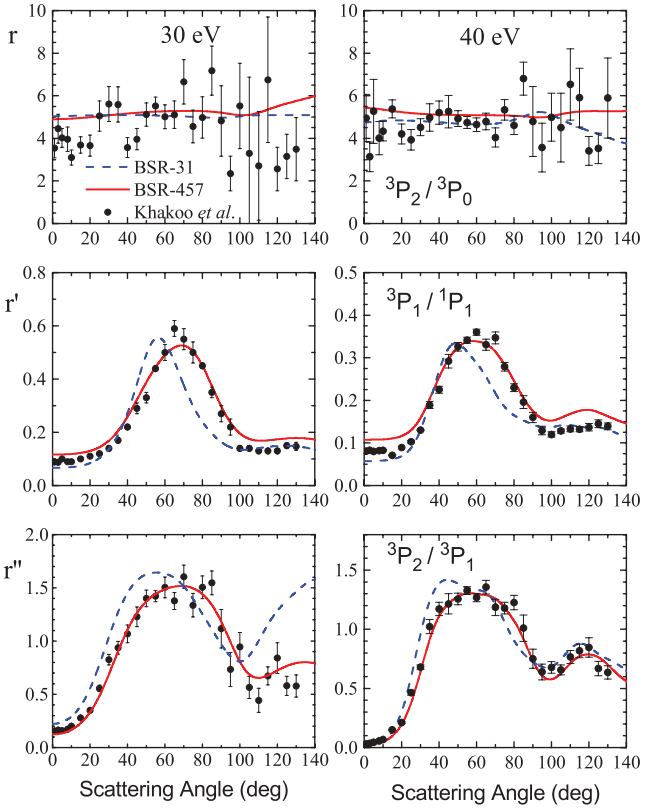

FIG. 9. (Color online) Angle-differential cross-section ratios r, r', and r'' (see the text for their definition) for electron-impact excitation of the $2p^5 3s$ states in neon from the ground state $(2p^6)^1S_0$ at incident projectile energies of 30 and 40 eV. The current BSR-457 results are compared with those from the earlier BSR-31 model [6] and the experimental data of Khakoo *et al.* [4].

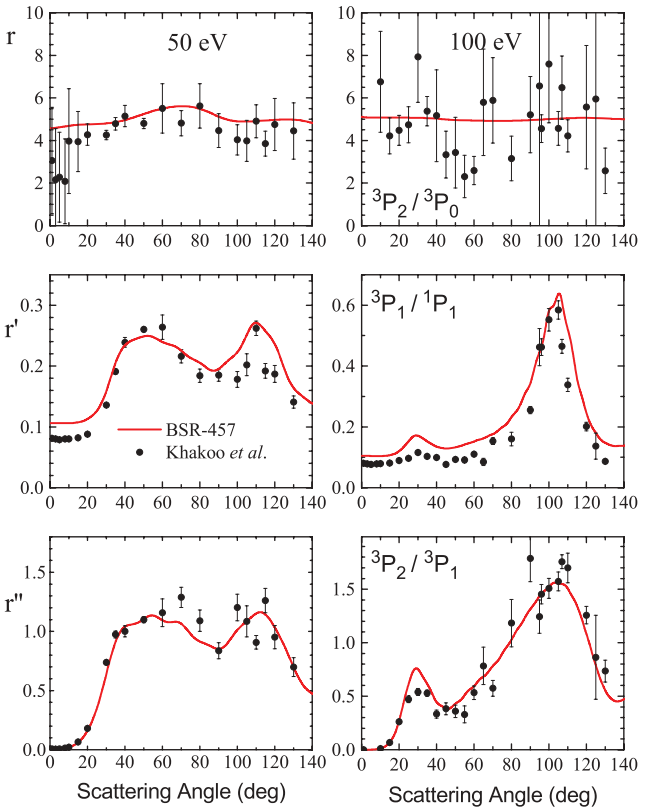

FIG. 10. (Color online) Same as Fig. 9 for incident projectile energies of 50 and 100 eV.

seems particularly challenging at 100 eV, where r reflects the ratio of two generally small numbers. Recall that these are both optically forbidden transitions with small cross sections at high incident energies.

The ratio r', which essentially reflects the contribution of exchange versus direct excitation, exhibits a well-defined structure. Our BSR-457 model accurately reproduces both the position and the magnitude of the peaks and represents a clear improvement over the earlier BSR-31 calculation. The r'' parameter measures the strength of the metastable excitation channels relative to the allowed channels. It exhibits the most complicated angular dependence, which is again accurately reproduced in the present scattering model over the entire angular range.

In summary, the BSR-457 ratios provide considerable improvement over all previous theoretical predictions presented by Khakoo *et al.* [4] (not shown here for clarity of the panels). The only significant discrepancy with experiment occurs at small scattering angles for the ratio r'. The small-angle results for this ratio are essentially determined by the ratio of the oscillator strengths for transitions between the states of interest. As mentioned above, our $3s[3/2]_1$ oscillator strength is 20% higher than the recommended value, and hence our r' ratios exceed experiment at small angles by a factor of about 1.2. Nevertheless, the predicted angular dependence is very satisfactory.

IV. CONCLUSIONS AND OUTLOOK

We carried out large-scale R-matrix with pseudostates calculations for electron scattering from neon in the intermediate-coupling scheme. The present work provides individual state-to-state results for excitation and thereby extends our recent nonrelativistic LS-coupling calculations [13]. The latter were intended to provide accurate cross sections for elastic scattering, the sum of all excitation processes, ionization, and the grand total cross section, respectively.

The present calculations were carried out with a recently developed parallel version of the BSR suite of computer programs [5]. Our results confirm an earlier prediction [10] regarding a very strong influence of coupling to the target continuum in calculating excitation cross sections for e-Ne collisions, even for strong dipole-allowed transitions. Comparison with available experimental data and with previous calculations raises questions about the absolute normalization of the excitation cross sections in the existing data sets. Our calculations generally predict significantly smaller cross sections at intermediate energies from threshold up to about 100 eV than the data used in many applications. Even for strong resonance excitation of the $2p^5 3s$ ($J = 1$) levels, the corrections due to coupling to the continuum were occasionally as large as a factor of 2. More profound effects were found for excitation of the $2p^5 3p$ and $2p^5 3d$ levels, where the corrections reached factors of up to 5. Note that coupling to the continuum and the high-lying Rydberg states was found to be important also at relatively low energies below the ionization threshold.

At the same time, the present calculations considerably improved the agreement with the experimental angular dependence of the differential cross sections. In particular, we resolved the long-standing discrepancy between experiment and theory for the DCS in exciting the metastable levels of neon. These predictions are very sensitive to the details of the scattering model, and the present results confirm that the earlier discrepancy is due to the slow convergence of the close-coupling expansion in these cases. We also obtained very good agreement with experiment for the cross-section ratios, which are very sensitive parameters to test the collision model.

The results reported in this paper are available in electronic format upon request. We believe that these cross sections considerably improve and extend the existing database for e-Ne collisions. Given the remaining discrepancies with absolute experimental data for some excitation cross sections, further measurements with accurate absolute normalization are highly desirable. In the future we plan to carry out similarly extensive calculations for Ar, Kr, and Xe. The latter will require a parallelized fully relativistic version of the BSR codes. Work in this direction is currently in progress.

ACKNOWLEDGMENTS

This work was supported by the United States National Science Foundation under Grants No. PHY-0903818, No. PHY-1068140, and No. PHY-1212450, and by the XSEDE supercomputer allocation TG-PHY090031. All calculations were carried out on Ranger and Lonestar at the Texas Advanced Computer Center.

[1] V. Zeman and K. Bartschat, J. Phys. B **30**, 4609 (1997).
[2] J. E. Chilton, M. D. Stewart, and C. C. Lin, Phys. Rev. A **61**, 052708 (2000).
[3] J. B. Boffard, M. L. Keeler, G. A. Piech, L. W. Anderson, and C. C. Lin, Phys. Rev. A **64**, 032708 (2001).
[4] M. A. Khakoo, J. Wrkich, M. Larsen, G. Kleiban, I. Kanik, S. Trajmar, M. J. Brunger, P. J. O. Teubner, A. Crowe, D. J. Fontes, R. E. H. Clark, V. Zeman, K. Bartschat, D. H. Madison, R. Srivastava, and A. D. Stauffer, Phys. Rev. A **65**, 062711 (2002).
[5] O. Zatsarinny, Comput. Phys. Commun. **174**, 273 (2006).
[6] O. Zatsarinny and K. Bartschat, J. Phys. B **37**, 2173 (2004).
[7] J. Bömmels, K. Franz, T. H. Hoffmann, A. Gopalan, O. Zatsarinny, K. Bartschat, M.-W. Ruf, and H. Hotop, Phys. Rev. A **71**, 012704 (2005).
[8] M. Allan, O. Zatsarinny, and K. Bartschat, Phys. Rev. A **74**, 030701 (2006).
[9] M. Allan, K. Franz, H. Hotop, O. Zatsarinny, and K. Bartschat, J. Phys. B **42**, 044009 (2009).
[10] C. P. Ballance and D. C. Griffin, J. Phys. B **37**, 2943 (2004).
[11] D. Dodt, A. Dinklage, R. Fischer, K. Bartschat, O. Zatsarinny, and D. Loffhagen, J. Phys. D **41**, 205207 (2008).
[12] D. Dodt, A. Dinklage, K. Bartschat, and O. Zatsarinny, New J. Phys. **12**, 073018 (2010).
[13] O. Zatsarinny and K. Bartschat, Phys. Rev. A **85**, 062710 (2012).
[14] R. D. Cowan, *The Theory of Atomic Structure and Spectra* (University of California, Berkeley, 1981).
[15] O. Zatsarinny and C. Froese Fischer, Comput. Phys. Commun. **180**, 2041 (2009).
[16] O. Zatsarinny and K. Bartschat, Phys. Scr. **T134**, 014020 (2009).
[17] Yu. Ralchenko *et al.*, *NIST Atomic Spectra Database* (version 5); http://www.nist.gov/pml/data/asd.cfm (National Institute of Standards and Technology, Gaithersburg, 2012).
[18] Z. P. Zhong, S. L. Wu, R. F. Feng, B. X. Yang, Q. Ji, K. Z. Xu, Y. Zou, and J.-M. Li, Phys. Rev. A **55**, 3388 (1997).
[19] N. Badnell, J. Phys. B **32**, 5583 (1999); See also http://amdpp.phys.strath.ac.uk/UK_RmaX/codes.html.
[20] L. R. Hargreaves, C. Campbell, M. A. Khakoo, O. Zatsarinny, and K. Bartschat, Phys. Rev. A **85**, 050701 (2012).
[21] D. F. Register, S. Trajmar, G. Steffensen, and D. C. Cartwright, Phys. Rev. A **29**, 1793 (1984).
[22] M. H. Phillips, L. W. Anderson, and C. C. Lin, Phys. Rev. A **32**, 2117 (1985).
[23] T. Y. Suzuki, H. Suzuki, S. Ohtani, B. S. Min, T. Takayanagi, and K. Wakiya, Phys. Rev. A **49**, 4578 (1994).
[24] H. Kato, M. Hoshino, H. Tanaka, and M. J. Brunger (private communication).